GA–A24007

PHYSICS PROCESSES IN DISRUPTION MITIGATION USING MASSIVE NOBLE GAS INJECTION

by
D.A. HUMPHREYS, D.G. WHYTE, T.C. JERNIGAN, T.E. EVANS,
D.S. GRAY, E.M. HOLLMANN, A.W. HYATT, A.G. KELLMAN,
C.J. LASNIER, P.B. PARKS, and P.L. TAYLOR

JULY 2002

DISCLAIMER

PHYSICS PROCESSES IN DISRUPTION MITIGATION USING MASSIVE NOBLE GAS INJECTION

by

D.A. HUMPHREYS, D.G. WHYTE,[†] T.C. JERNIGAN,[‡] T.E. EVANS,
D.S. GRAY,[†] E.M. HOLLMANN,[†] A.W. HYATT, A.G. KELLMAN,
C.J. LASNIER,[△] P.B. PARKS, and P.L. TAYLOR

[†]University of California, San Diego
[‡]Oak Ridge National Laboratory
[△]Lawrence Livermore National Laboratory

Physics Processes in Disruption Mitigation Using Massive Noble Gas Injection

D.A. Humphreys,[1] D.G. Whyte,[2] T.C. Jernigan,[3] T.E. Evans,[1] D.S. Gray,[2] E.M. Hollmann,[2] A.W. Hyatt,[1] A.G. Kellman,[1] C.J. Lasnier,[4] P.B. Parks,[1] and P.L. Taylor[1]

[1]*General Atomics, P.O. Box 85608, San Diego, California 92186-5608 USA*
[2]*University of California, San Diego, 9500 Gilman Drive, La Jolla, California 92093 USA*
[3]*Oak Ridge National Laboratory, P.O. Box 2008, Oak Ridge, Tennessee 37831*
[4]*Lawrence Livermore National Laboratory, P.O. Box 808, Livermore, California 94551 USA*

I. INTRODUCTION

Methods for detecting imminent disruptions and mitigating disruption effects using massive injection of noble gases (He, Ne, or Ar) have been demonstrated on the DIII–D tokamak [1]. A jet of high injected gas density ($> 10^{24}$ m^{-3}) and pressure (> 20 kPa) penetrates the target plasma at the gas sound speed (~300–500 m/s) and increases the atom/ion content of the plasma by a factor of > 50 in several milliseconds. UV line radiation from the impurity species distributes the plasma energy uniformly on the first wall, reducing the thermal load to the divertor by a factor of 10. Runaway electrons are almost completely eliminated by the large density of free and bound electrons supplied by the gas injection. The small vertical plasma displacement before current quench and high ratio of current decay rate to vertical growth rate result in a 75% reduction in peak halo current amplitude and attendant forces.

II. DISRUPTION EFFECTS, DETECTION, AND MITIGATION

A vertical displacement event (VDE) disruption is characterized by an initial loss of vertical position, followed by wall limiting, a drop in edge safety factor, and finally a plasma-terminating thermal quench. A major disruption by contrast occurs when the plasma stored energy is lost before any loss in plasma position. Both can apply a large thermal load to plasma facing components (PFC's), particularly near the divertor strikepoints or the limiting point. Because motion into a limiting surface converts currents on closed field lines to current on open (halo) field lines with high efficiency, a VDE tends to produce the largest halo currents [2]. Finally, the large electric fields produced during a rapid current quench in the very cold (typically $T_e < 30$ eV in DIII-D) post-thermal quench plasma can exceed the critical field required to produce runaway electrons [3].

High performance next-generation devices as well as power reactors will require reliable and accurate disruption detection algorithms, coupled with a robust and effective mitigation method. In DIII-D the imminent onset of a variety of disruptions can be detected by a variety of physics-based recognition algorithms implemented in the DIII-D Plasma Control System (PCS) [4], which can take corrective action or trigger the gas injection mitigation system in response. Figure 1 illustrates the use of a vertical position threshold detector in identifying an intentionally-induced VDE and triggering the mitigation system. Following disabling of vertical control, the plasma moves downward and crosses the specified threshold vertical position (± 5 cm). The PCS generates a signal triggering injection of high pressure Ne, which produces a radiative thermal quench ~4 ms after the trigger. Only 3%–5% of the total plasma (thermal and magnetic) energy is conducted to the divertor surface in a mitigated disruption, while typically 20%–40% is delivered to the divertor in an unmitigated disruption. Peak stress from halo currents is reduced by ~75% from the unmitigated value.

Other detection algorithms implemented in the PCS include a radiated power threshold and a sophisticated neoclassical tearing mode (NTM) and locked mode detector.

High pressure impurity gas injection significantly mitigates all of the principal disruption effects in DIII-D and offers a promising option for disruption mitigation in burning plasma experiments. The DIII-D high pressure impurity gas injection system consists of a 7 MPa reservoir which can inject $\sim 4\times 10^{22}$ particles into the vessel in 2–5 ms using a fast-opening valve. If distributed uniformly throughout the 20 m^3 of the DIII-D plasma volume, this yields an impurity density of $\sim 2\times 10^{21}$ particles/m^3, > 50 times the initial plasma density. The
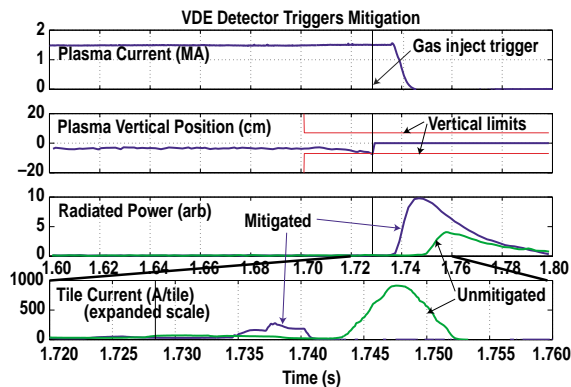

Fig. 1. Illustration of vertical position threshold detector used to identify an intentionally-induced VDE and trigger the impurity gas injection system.
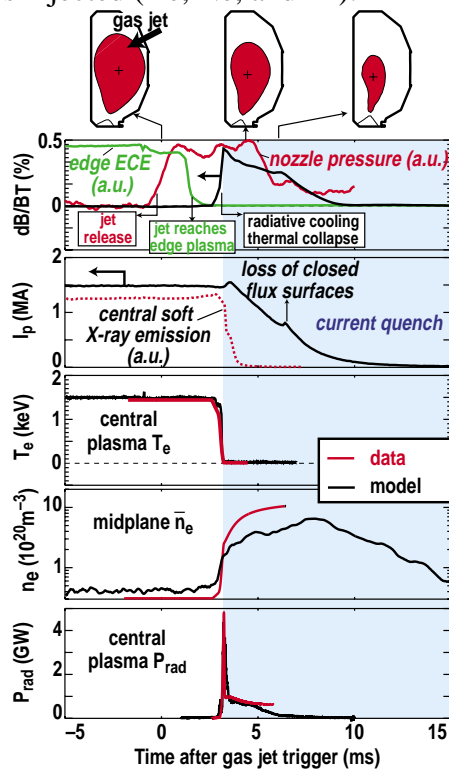
ram pressure produced by the jet is typically 20–30 kPa, several times larger than the volume-averaged plasma electron pressure (~ 7 kPa) and comparable to the peak plasma pressure in the DIII-D target plasmas studied. That the jet pressure is significantly greater than the plasma pressure is supported by the observation that the propagation of the cold front is ballistic at the sound velocity of each impurity species injected (He, Ne, and Ar).

The KPRAD code [5] makes use of power balance and detailed accounting of impurity and target species ionization states to predict the evolution of the thermal collapse, including T_e, Z_{eff}, and densities of ionized and neutral impurities. Figure 2 shows an example of a KPRAD calculation for a He-mitigated disruption in which a VDE is not triggered and the final plasma T_e equilibrates at ~ 3.4 eV during the current quench. Virtually 100% of the plasma stored energy is radiated isotropically by the impurity, principally as UV line radiation, in a thermal quench of less than 0.1 ms [1]. The plasma remains well-centered in the absence of a forced VDE, resulting in a very low peak halo current fraction (peak poloidal halo current $\sim 0.07 I_{p0}$) when the plasma eventually limits against the divertor floor. Good agreement is seen between experimental and modeled evolution of the plasma electron temperature and density, as well as total radiated power and current decay rate.

Fig. 2. KPRAD simulation of pre-emptive termination using high pressure He-gas injection.

The detailed evolution of both core and halo plasmas can be simulated with significant accuracy using the GA halo model [1] and plasma geometry evolution data reconstructed by the JFIT code [6]. One key result of this model is that the peak poloidal halo current in a VDE is reduced by increasing the post-thermal quench plasma resistivity or by decreasing the plasma velocity during the wall-limited phase of the VDE. These actions will produce a higher halo safety factor during the current quench, and thus reduce the poloidal halo current since the poloidal halo current is inversely proportional to the instantaneous halo safety

factor, $I_{halo}^{pol} = I_{halo}^{tor}/q_{halo}$. The toroidal halo current, I_{halo}^{tor}, is proportional to the plasma current at the beginning of the wall-contact phase of the current quench.

Mitigation of disruption halo currents by early injection of high-pressure impurity gas occurs primarily by reducing the plasma current at the beginning of the wall-contact phase of the current quench by initiating the current quench well before the plasma is wall-limited, ideally before any vertical motion has begun. Figure 3 shows an example of the halo model applied to a comparison of mitigated and unmitigated VDE's. The mitigated case corresponds to

Fig. 3. Application of halo model to unmitigated (a) and mitigated (b) discharges shows good agreement for T_e(unmitigated)=5 eV, Z_{eff}(unmitigated)=1.5, T_e(mitigated)= 2.4 eV, Z_{eff}(mitigated)=1.5.

injection of high-pressure Ne gas when the plasma has moved ~5 cm from its equilibrium position. These simulations show that the unmitigated case is consistent with post-thermal quench values of T_e ~5.0±0.5 eV, Z_{eff} =1.5, while the mitigated case is consistent with post-thermal quench values of T_e ~2.4±0.5 eV, Z_{eff}=1.5 (and thus increased resistivity).

To explore the importance of prompt mitigation, a set of DIII-D experiments was performed in which the VDE detector was used to vary the vertical position at which the gas injection occurred. Figure 4 shows the peak halo current and toroidal peaking factor (TPF) measured as a function of the vertical position at time of mitigation. The figure shows that the peak halo current is larger the later into the VDE the gas is fired. Figure 5 shows a series of trajectories in the phase space of plasma current $I_p(t)$ versus vertical

Fig. 4. Peak halo current and TPF as a function of vertical position at which gas injection occurs.

position $Z_p(t)$. The line indicating the vertical position at the point of wall contact is crossed at increasingly high values of plasma current with later times of gas injection. The results support the model that the halo current is proportional to the plasma current at the time when the plasma is both in wall contact and undergoing the current quench. The larger plasma minor radius and thus halo safety factor at wall contact further serves to reduce the poloidal component of the halo current.

Runaway electrons can be generated when the large parallel electric field ($E_∥$) produced by the high resistive loop voltage (typically V_L^{CQ} ~ 500–1000 V in DIII-D) in the post-thermal quench plasma accelerates electrons to relativistic speeds. If $E_∥ > E_{crit} \equiv mc\nu/e$ αn_e(thermal), the acceleration will exceed the collisional drag, allowing any seed relativistic electrons to experience knock-on avalanche amplification to become a population of runaway electrons. The collisional slowing-down rate ν is proportional to the thermal electron density, including both bound and unbound electrons. The amplification is $\propto e^G$, where $G \equiv \gamma_{RE}\tau_{CQ}$, and $\gamma_{RE} \propto \nu(E_∥/E_{crit} - 1)$. Thus, a sufficiently large total (bound+unbound) thermal electron density will yield $E_{crit} > E_∥$ so that $\gamma_{RE} < 0$, and there will be no runaway amplification. Injection of massive impurity gas density nearly satisfies this constraint in DIII-D, and no runaways are observed under mitigation.
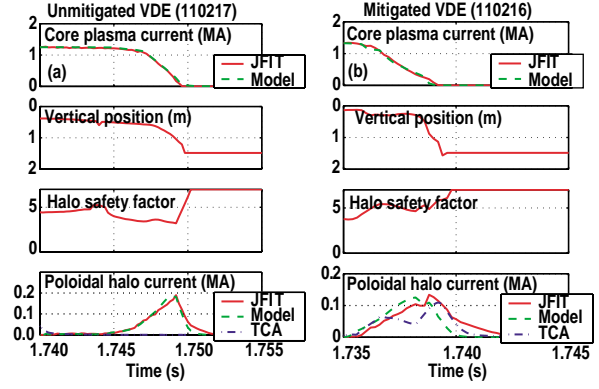
III. EXTRAPOLATION OF MITIGATION SCENARIOS TO BURNING PLASMA DEVICES

KPRAD simulations show that given sufficient penetration, an ITER-FEAT plasma can be brought down to $T_e \sim 1.5$ eV, with $Z_{eff} \sim 1.0$ using an Ar jet at ~30 kPa (a modest factor of 4–5 over the DIII-D value). Results of halo model simulations of ITER-FEAT disruption loads are summarized in Fig. 6, showing that the stress resulting from poloidal halo current alone in such a case is reduced by more than 75% from the unmitigated value (resulting from $T_e^{halo} = 20$ eV, $Z_{eff}^{halo} = 1.0$). A TPF of 2 was assumed for the unmitigated case, while unity was assumed for the mitigated case. A similar reduction in TPF is consistently seen in DIII-D mitigation by all species of impurity gas injection (see Fig. 4).

V. CONCLUSIONS

Most of the key processes of disruption effects mitigation are now well-understood. Models based on this understanding can be confidently applied to mitigation scenarios for next-generation devices, with certain caveats. In particular, mechanisms governing jet penetration in reactor-grade plasmas and the physics of halo width and geometry evolution remain to be well understood. High pressure gas injection is nevertheless an excellent candidate for simultaneous mitigation of all damaging disruption effects, with potential for high reliability at a relatively low cost. Experiments using physics-based disruption detection algorithms in the PCS to trigger the gas injection system in DIII-D demonstrate the effectiveness of this integrated approach.
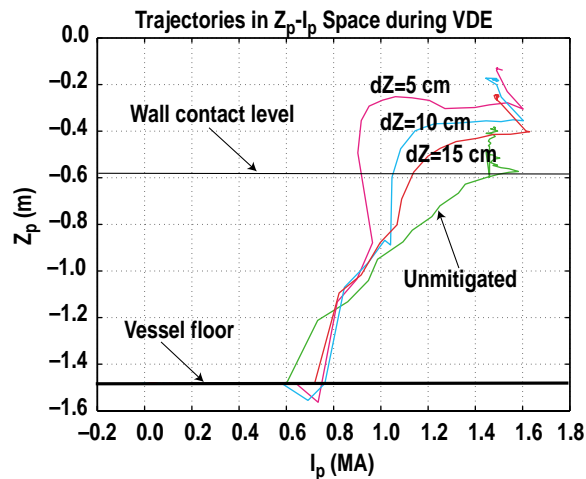

Fig. 5. Trajectories in Z-I_p space for varying vertical positions at which gas injection occurs. The fraction of plasma current lost by the time of wall-impact is greater the earlier the injection is performed.
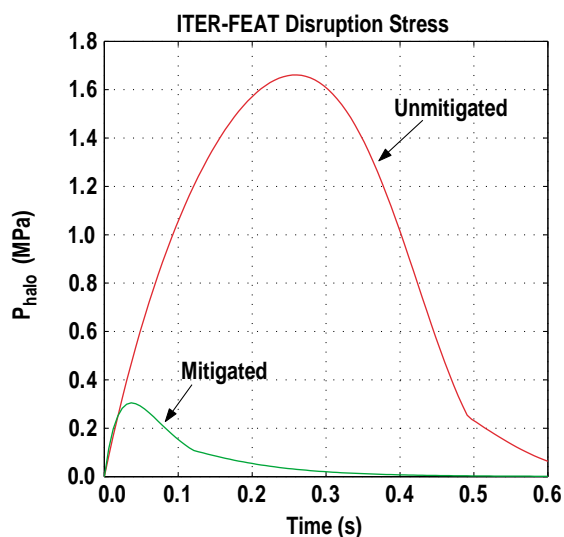

Fig. 6. Simulations of mitigated and unmitigated disruptions in ITER-FEAT show a dramatic potential reduction in halo current stress with impurity gas injection.

[1] D.G. Whyte, et al., "Mitigation of Tokamak Disruptions Using High-Pressure Gas Injection," submitted for publication in Phys. Rev. Letters, April 2002.
[2] D.A. Humphreys, A.G. Kellman, Phys. of Plasmas **6** (1999) 2742.
[3] M.N. Rosenbluth, et al., Nucl. Fus **37** (1997) 955.
[4] J.R. Ferron, et al., Proc. 24rd Conf. on Contr. Fusion and Plasma Phys., Berchtesgaden, Germany, 1997 (European Physical Society, Petit-Lancy, Switzerland)
[5] D.G. Whyte, et al., Proc. 24th European Physical Society Conference on Controlled Fusion and Plasma Physics, Berchtesgaden, Germany, 9-14 June 1997, Vol. **21A**, p. 1137.
[6] D.A. Humphreys, and D.G. Whyte, Phys. of Plasmas **7** (2000) 4057.